Diogo Miguel Monteiro Canhoto

Effect of chronic hyperglycaemia on β-catenin levels of hippocampal immature neurons from an Alzheimer's disease mouse model

Dissertation for the attainment of the Master in Medicine, under the supervision of Professor Ana Cristina Carvalho Rego[a,b] and Elisabete Baptista Ferreiro, PhD[a], submitted to the Faculty of Medicine, University of Coimbra, Portugal

· U C ·

UNIVERSIDADE DE COIMBRA

a. Center for Neuroscience and Cell Biology, University of Coimbra, Rua Larga, 3004-504 Coimbra, Portugal
b. Faculty of Medicine, University of Coimbra, Azinhaga de Santa Comba, Celas Polo III, 3000-354 Coimbra, Portugal

E-mail adresses: arego@fmed.uc.pt, a.cristina.rego@gmail.com (A.C. Rego), beferreiro@gmail.com (E.B. Ferreiro), diogo.mcanhoto@gmail.com (D.M. Canhoto)

Abstract

Alzheimer's disease (AD) is the leading cause of dementia in Western countries and the most prevalent neurodegenerative disease, still lacking efficacious treatment. Glucose dysmetabolism is believed to be a premature event in AD and unpublished data obtained by our group suggest that hyperglycaemia induces an exacerbation of the decline in adult hippocampal neurogenesis that occurs in AD. The Wnt/β-catenin pathway, believed to be dysfunctional in AD, is pivotal in adult hippocampal neurogenesis. β-catenin itself is essencial for neuronal function, impacts cell cycle regulation and has profound influence on dendritic morphogenesis. Therefore, we hypothesized a dysfunction of the Wnt/β-catenin pathway in the context of AD and simultaneous glucidic metabolic derrangement. Through this work we investigated the possibility of an influence of β-catenin following the superimposition of an AD phenotype and a diabetes-like state on adult hippocampal neurogenesis. To pursue this endeavour, chronic hyperglycaemia was induced in 2 month-old triple transgenic (3xTg-AD) male mice through a 6-month treatment with high-dose sucrose, and the presence of a diabetes-like syndrome confirmed through metabolic characterisation. Levels of total β-catenin were quantified in the nuclei, cytosol and processes of neuroblasts or dendrites of immature neurons and mature neurons of the hippocampal dentate gyrus, and their nuclear to cytosol ratios of β-catenin levels calculated. This analysis was reproduced in untreated 2 month-old 3xTg-AD and in non-transgenic animals to evaluate the influence of age on total β-catenin levels and their nuclear to cytosol ratios. Main findings consisted of a predominantly cytosolic distribution of β-catenin in neuroblasts and immature neurons of 2 month-old 3xTg-AD mice, when compared with the other experimental groups. Importantly, chronic hyperglycaemia lead to a redistribution of β-catenin, namely an accumulation in the nucleus of immature neurons of 8 month-old 3xTg-AD mice, when compared to the age-

matched untreated transgenic mice. These results substantiate the hypothesis that, along age, β-catenin accumulates in the nuclei of the neuroblasts and immature hippocampal neurons. When the effects of AD pathology and chronic hyperglycaemia were compounded, synergistic exacerbation of β-catenin accumulation in the nuclei of immature neurons possibly reflects a compensatory upregulation of β-catenin transcriptional activity, acting against the depletion of the precursor population of hippocampal neurons. Future investigations could be devoted to address the molecular mechanisms underlying the preferential nuclear distribution of β-catenin under the influence of 3xTg-AD genotype and diabetes-like phenotype.

Keywords: 3xTg-AD mice, Alzheimer's disease, β-catenin, dentate gyrus, hyperglycaemia, neurogenesis.

Resumo

A doença de Alzheimer (DA) é a principal causa de demência no mundo ocidental e a doença neurodegenerativa mais prevalente, para a qual escasseia ainda tratamento eficaz. A via metabólica Wnt/β-catenina, que se acredita estar disfuncional na DA, desempenha um papel primordial na neurogénese hipocampal no adulto. A β-catenina, por si só, é essencial para a função neuronal, tem influência na regulação do ciclo celular, e na morfogénese dendrítica. Evidências apontam para uma exacerbação do declínio da neurogénese adulta hipocampal verificada na DA, resultante de uma alteração do metabolismo glucídico, um evento prematuro nesta doença. Postulamos que a disfunção da via Wnt/β-catenina esteja exacerbada no contexto da DA e do distúrbio do metabolismo glucídico concomitante. Neste trabalho investigámos a influência das alterações metabólicas associadas à diabetes no fenótipo da DA nas alterações dos níveis totais de β-catenina de células envolvidas na neurogénese hipocampal no adulto, tais como neuroblastos e neurónios imaturos. Tendo em conta este objectivo, a hiperglicémia crónica foi induzida no murganho triplo transgénico (3xTg-AD) macho de 2 meses de idade através da administração de doses elevadas de sacarose durante um período de 6 meses, e a presença de um síndrome semelhante à diabetes corroborada pela caracterização metabólica destes animais. Os níveis de β-catenina total foram quantificados no núcleo, citosol e processos de neuroblastos e dendrites de neurónios imaturos e neurónios maduros da camada granular do giro dentado hipocampal. Por forma a avaliar a distribuição celular e a predominância nuclear deste factor de transcrição, foram determinados os rácios de β-catenina entre o núcleo e o citosol das referidas células. Esta análise foi reproduzida em animais 3xTg-AD de dois meses de idade e em animais não transgénicos no sentido de avaliar a influência da idade nestes parâmetros. Os resultados demonstraram que, aos 2 meses de idade, a β-catenina se encontrava principalmente localizada ao citosol de neuroblastos e

neurónios imaturos hipocampais dos animais 3xTg-AD, em comparação com os restantes grupos experimentais. A hiperglicémia crónica levou a uma redistribuição da β-catenina, nomeadamente a uma acumulação nuclear em neurónios imaturos de animais 3xTg-AD com 8 meses de idade quando comparados com os animais da mesma idade não tratados com sacarose. Estes resultados corrobooram a hipótese de que, com o envelhecimento, a β-catenina se acumula nos núcleos dos neuroblastos e neurónios imaturos hipocampais. A acumulação de β-catenina no núcleo dos neurónios imaturos por efeito sinergístico da patologia da DA, da hiperglicémia crónica e da idade poderá traduzir uma sobre-regulação compensatória da actividade transcripcional da β-catenina, que actuaria contra a depleção da população precursora dos neurónios hipocampais. Investigações futuras poderão ser dedicadas a identificar os mecanismos moleculares subjacentes à distribuição nuclear preferencial da β-catenina sob a influência do genótipo 3xTg-AD sujeito a uma condição semelhante à diabetes.

Palavras-chave: β-catenina, doença de Alzheimer, giro dentado, hiperglicémia, murganho 3xTg-AD, neurogénese.

Table of contents

List of abbreviations

3xTg-AD	triple transgenic mouse model of Alzheimer's disease
AD	Alzheimer's disease
AGE	advanced glycation end-product
ANOVA	analysis of variance
APC	adenomatous poliposis coli
AUC	area under the curve
Aβ	β-amyloid
Aβ-AGE	β-amyloid advanced glycation end-product
BCL9	B-cell CLL/lymphoma 9
BSA	bovine serum albumin
CA3	*cornus ammonis* 3
DCX	doublecortin
DG	dentate gyrus
GCL	granule cell layer
GSK-3β	glycogen synthase kinase-3β
GTT	glucose tolerance test
IDA	integrated density per area
MAP2	microtubule-associated protein 2
ML	molecular layer
NonTg	non-transgenic
NSPCs	neural stem/progenitor cells
OCT	optimal cutting temperature compound
PBS	phosphate buffered saline

PFA	paraphormaldehyde
RAGE	receptor for advanced glycation end-products
ROI	region of interest
RT	room temperature
SEM	standard error of the mean
SGZ	subgranular zone
T2D	type 2 diabetes
T3D	type 3 diabetes
TCF4	transcription factor 4

1. Introduction

Alzheimer's disease (AD) is the most prevalent neurodegenerative illness and the commonest form of senile dementia [1]. AD is clinically manifested through a primary deterioration of the patient's work memory, which relentlessly progresses to impact the remaining mental faculties. Available treatments are moderately efficacious and are generally considered of palliative nature. The societal burden of the illness is compounded by its toll on family and caregivers [2], thus rendering the need for the identification of additional therapeutic targets even more necessary.

Neuropathological hallmarks of AD include extracellular senile plaques, resultant of β-amyloid (Aβ) peptide overproduction and aggregation, intraneuronal neurofibrillary tangles, formed by aggregation of hyperphosphorylated tau protein, activation of microglia, and neuronal and synaptic loss [3]. These pathological features contribute to the loss of normal neural function in the hippocampus, a brain region intricately associated with AD manifestations, namely memory impairment [4].

Type 2 diabetes (T2D) is a pathological state of glucose dysmetabolism, insulin resistance and resulting chronic hyperglycaemia. T2D is a known risk factor for AD and is believed to be involved in its pathogenesis, as both diseases share pathophysiological traits, including oxidative stress, pro-inflammatory states and brain microvascular disease [5-9]. Furthermore, under hyperglycaemic conditions, the rate at which Aβ reacts non-enzymatically with glucose is faster, yielding Aβ-AGE, an advanced glycation end-product (AGE) of greater neurotoxicity, and also an upregulator of Aβ production [10]. The proximity between the two conditions lead to the emergence of the concept of type 3 diabetes (T3D), which views AD as a form of diabetes with particular selectivity for the brain [8].

Adult neurogenesis consists of the newly production of functional neurons, occurring in distinct areas of the mammalian adult brain, termed neurogenic niches [4,11]. One neurogenic niche is situated at the subgranular zone (SGZ) of the dentate gyrus (DG) located in the hippocampus. In the SGZ, neural stem/progenitor cells (NSPCs) divide to generate granule cells, which, upon differentiation, migrate from the SGZ to the granule cell layer (GCL) of the DG [12], where they grow an axonal process to *Cornu Ammonis* area 3 (CA3) and apical dendrites to the molecular layer (ML), being integrated into pre-existing neural circuitry [13]. This takes place in a strictly regulated milieu in the vicinity of vasculature [4,14]. Regulatory cues derived from the surrounding cells partake in the (i) modulation of precursor cell proliferation, (ii) selection of progeny through apoptosis, (iii) postmitotic differentiation, including alterations in dendritic arborization, activity, and number of dendritic spines, and (iv) integration into the pre-existing neuronal network [12].

Adult hippocampal neurogenesis is thought to play an important role in memory formation and preservation [15,16] and its disruption has been linked to AD [17]. One pathway involved in adult neurogenesis that is dysfunctional in AD is the Wnt signalling pathway, which has been proposed as being protective against synaptic loss in AD [4,18], as well as acting as a mediator in dendrite formation, upkeep and function [4]. In the hippocampus of AD patients, dysfunctional Wnt signalling is promoted by increased glucogen synthase kinase-3β (GSK-3β) activity [4,19,20], resulting in proteasomal degradation of β-catenin, one of the downstream mediators of the pathway [4]. β-catenin activity correlates with the extent of arborization of dendritic trees in hippocampal neurons [21] and is a necessary factor for correct dendritic morphogenesis [22]. GSK-3β is activated by Aβ-AGE through its interaction with the receptor for advanced glycation end-products (RAGE) [10]. For this reason, enhanced stimulation of this receptor under conditions of

chronic hyperglycaemia culminates in the establishment of a positive feedback loop, ultimately inhibiting the Wnt pathway [4].

Because the impact of chronic hyperglycaemia-induced downregulation of the Wnt pathway on adult hippocampal neurogenesis remains largely unknown, comparative experiments were carried out in 2 and 8 month-old triple transgenic (3xTg-AD) animals to evaluate age-related changes in β-catenin levels, which showed a lesser nuclear to cytosolic ratio in neuroblasts of the 2 month-old non-transgenic and 3xTg-AD animals and in immature neurons of the 3xTg-AD animals of the same age. Evaluation of nuclear and cytosolic β-catenin levels in neuroblasts and immature neurons in the granular cell layer of the dentate gyrus from 3xTg-AD mice subjected to chronic hyperglycaemia revealed increased nuclear to cytosolic ratio in β-catenin levels. Analysis of β-catenin levels and its cellular distribution in hippocampal neuronal precursors and mature neurons remained, to the date, a gap in the knowledge in the field of hippocampal neurogenesis. This study integrates these findings in the context of two oft-comorbid factors, AD pathology and diabetes-like phenotype.

2. Materials and methods

2.1. Ethics statements

All animal procedures were performed with approval of the local institutional animal care committee and animal house (Biotério FMUC; License nº 520.000.000.2006) and abbided by the local ('Decreto-Lei nº113/2013') and European (European Community Council Directive for the Care and Use of Laboratory Animals and European; European directive 2010/63/EU) animal welfare guidelines and legislation.

2.2. Animal care and treatment groups

Triple transgenic AD (3xTg-AD) male mice, carrying $PS1_{M146V}$, APP_{SWE} and tau_{P301L} mutations [23,24], and non-transgenic (NonTg) C57BL6/129S male mice, used as controls, were a courteous offer by Dr. Frank Laferla (Department of Neurobiology and Behavior and Institute for Brain Aging and Dementia, University of California, Irvine, USA). Animals were bred and housed at the CNC-Faculty of Medicine (University of Coimbra, Portugal) animal house, under conditions of constant temperature (20 ºC - 22 ºC), humidity (50 - 60% relative humidity) and according to an artificial photoperiod (from 7.00 a.m. to 7.00 p.m.).

Age-matched 3xTg-AD (n = 16) and NonTg (n = 16) animals were divided into 4 separate groups and caged in identical polycarbonate cages, containing a malleable paper bag that was changed twice a week. In order to simulate the chronic hyperglycaemic state of T2D patients, 2 month-old mice of the same genotype were divided into a group fed with 20 % (w/v) sucrose aquous solution and a water-fed group, during 6 months, as summarised in Table 1. Solutions were replaced three times per week as a pre-emptive measure against growth of pathogens. Animal ration (# 4RF21A, Mucedola, Milanese, Italy) was supplied *ad*

libitum. To allow for study of age-related changes, untreated 2-month-old animals of either genotype were additionally used.

Table 1. Experimental groups.

	Age (mo.)	Treatment	n	Designation
NonTg	2	Control	4	NonTg-2C
	8	Control	8	NonTg-8C
		Sucrose	8	NonTg-8Suc
3xTg-AD	2	Control	4	3xTg-AD-2C
	8	Control	8	3xTg-AD-8C
		Sucrose	8	3xTg-AD-8Suc

2.3. Characterisation of glucose metabolism

Intakes of water / sucrose and food were monitored throughout the duration of the study. Serial weightings of each animal were performed weekly using a digital scale (3 decimals).

A glucose tolerance test (GTT) was performed at 2 months of age to establish a baseline. Briefly, for the glucose tolerance tests, 3xTg-AD and NonTg mice were fasted overnight (12h) and injected intraperitoneally with a glucose load (2 g/kg of weight prepared in Milli-Q water). Serial glucose measurements were performed in whole-blood samples drawn from the tip of the tail with a hand-held whole-blood glucose monitor (Accu-Chek

Aviva device (Roche)) immediately before the glucose load and at 15, 30, 60 and 120 minutes post-injection. Prior to their sacrifice at 8 months of age, animals were weighted, a glucose tolerance test performed, and random and postprandial glucoses measured. For the postprandial and random glucose measurements, glucose levels were evaluated after two hours fasting, started immediately at the beginning of the light cycle, or occasionally during the light cycle, respectively.

2.4. Histological techniques

3xTg-AD and NonTg mice underwent profound anesthetisation through an intraperitoneal injection of sodium pentobarbital (70 mg/kg prepared in 0.9% NaCl). During the anesthetised state, a 4-minutes 0.9% NaCl perfusion was performed through intracardiac catheterization. Following the perfusion, the *crania* were dissected to extract the *encephalus*, which was divided sagitally into the two cerebral hemispheres and adjoining portions of the cerebellum and brain stem. These were fixed in 4% paraphormaldehyde (PFA) overnight. The fixated hemispheres were washed twice in phosphate buffered (pH 7.4) saline (PBS) (containing in mM: 137 NaCl, 2.7 KCl, 1.8 KH_2PO_4, 10 $Na_2HPO_4 \cdot 2H_2O$) and immersed in 30% (w/v) sucrose in PBS solution at 4 ºC until they sank, for dehydration and cryoprotection. The sunken brain tissues were frozen using liquid nitrogen and stored at -20 ºC until sectioning. Sectioning of the hemispheres was performed using a cryostate ((Leica Microsystems CM3050 S, Mannheim, Germany). Hemispheres were embedded in block of optimal cutting temperature compound (OCT) (Sakura), which provided the tissue the stability to withstand the movement of the blade and therefore prevented unwanted damage or striation of tissue. During the cutting procedure, chamber temperature was kept at -20 ºC and object temperatures at -22 ºC. Cryosections were obtained at 40 μm rostrocaudal coronal intervals. Slices were collected in six series and were stored at -20ºC in antifreezing solution

of 30% glycerol (v/v) and 30% polyethylene glycol (v/v) in 0.1 M phosphate buffer, pH 7.4). The cerebral hemispheres of the 2-month-old animals were obtained and preserved following the same procedures. In this case, sectioning was performed at a vibratome (Leica VT1200S, Mannheim, Germany). A 3% (m/v) solution of ultrapure™ low melting point agarose (#16520050, Thermofisher Scientific, Waltham, MA USA) in PBS was heated to liquidity and used to embed each cerebral hemisphere as it was left to solidify. Ice was used to speed solidification of the agarose and to preserve the tissue during both the processes of agarose block preparation and cutting. The agarose blocks containing the brain tissue were transferred and glued to the vibratome object. Sectioning was performed at 0.6 mm/s using a standard scalpel blade. The slices yielded through this process were of identical orientation of the ones obtained at the cryostate. The storage of the sections was the same as for the 8-month-old animals.

2.5. Fluorescent immunohistochemistry

Sections obtained from each animal were labelled for doublecortin (DCX) and microtubule-associated protein 2 (MAP2), which label neuronal precursor cells and mature neuronal cells, respectively. They were also labelled for β-catenin and with Hoechst 33342 to label the DNA (and hence the nuclei) of each cell. The free-floating sections from each of the animal groups were washed with PBS (3 x 10 min) and then incubated with blocking solution of PBS with 3% bovine serum albumin (BSA; Sigma Chemical Co., St. Louis, MO, USA) and 1% Triton X-100 for 1h at room temperature (RT). They were then incubated with primary antibodies against goat anti-DCX (1 : 500; Clone C-18, Sc-8066, Santa Cruz Biotechnologies), rabbit anti-β-catenin (1 : 500; # ab32572, abcam, Cambridge, UK) and chicken anti- MAP2 (1 : 2000; # ab92434, abcam, Cambridge, UK) diluted in the blocking solution, during 3 overnights at 4ºC. Sections were further washed with PBS (3 x 10 min) at

RT, in the dark and incubated for 1 h with Alexa Fluor® 568 donkey anti-goat (#A-11057) and Alexa Fluor® 488 donkey anti-rabbit (#A-21206). Slices were further blocked for 1 h with the blocking solution and incubated for 1 h with Aleca Fluor® 633 goat anti-chicken and Hoechst 33342 (1:10,000 from a stock of 2mg/ml; H1399, Thermofisher Scientific, Waltham, MA USA). Secondary antibodies were all used at a dilution of 1:1000 and were obtained from Thermofisher Scientific (Waltham, MA USA). Washing with PBS (3 x 10 min) was again performed and sections were transferred onto microscope slides and mounted with antifading medium (Fluoroshield Mounting Medium, # ab104135, Abcam).

2.6. Quantification of β-catenin levels

Single-plane confocal images were obtained from the slides (from bregma -1.70 mm to -3.52 mm) using a Carl Zeiss LSM 710 confocal microscope (Oberkochen, Germany). For each group, the number of images analysed were the following: NonTg-8C (105 images (n = 11-16/animal)); NonTg-8Suc (104 images (n = 10-15/animal)); and 3xTg-AD-8C (72 images (n = 9-17/animal)); 3xTg-AD-8Suc (82 images (n = 5-15/animal)). Concerning the 2-month-old animals, the following images were used: NonTg-2mo. (13 images (n = 6-7/animal)) and 3xTg-AD-2mo. (13 images (n =5-8/animal)).

The microscopy images were analysed using the image-processing package Fiji (version 51f) (http://fiji.sc/Fiji) [25]. A macro was designed to create regions of interest (ROIs), which comprised the nuclei, somata, and processes/dendrites of neuroblasts and immature neurons of the DG GCL, as well as the nuclei and dendrites of mature neuronal cells of DG GCL. A second macro was then developed to subtract the nucleus ROI from the soma ROI for the neuroblasts and immature neurons, thereby allowing quantification of β-catenin in the cytosol. Mature neurons are abundant in the DG GCL and located in close proximity to one another, thereby making it impossible to delineate their somata as in the

neuroblasts and immature neurons. To circunvent this problem, another macro was used to create a 6-pixel-wide band around the nucleus, thus allowing sampling of the cytosol for the quantification of the mean integrated density of β-catenin/cytosol area.

A final macro was designed to quantify the mean integrated density of β-catenin signals, determined at all possible thresholds and divided by the respective area. The mean integrated density per area (IDA) of β-catenin for each ROI type were averaged for each animal. For the analysis of the distribution pattern of β-catenin to the nucleus total β-catenin signal was quantified in each region, for each possible thresholds using the same macro as before, and a ratio applied between nucleus and cytosol integrated density.

2.7. Statistical analysis

Data from this study were analysed by using GraphPad Prism 5.0 for MacIntosh (GraphPad Software Inc., San Diego, CA, USA) or Statistical Package for the Social Sciencs (SPSS) 22 softwares and were expressed as mean ± standard error of the mean (SEM). Comparisons were performed by repeated measures two-way analysis of variance (ANOVA), except for random and postprandial glycaemias, area under the blood glucose curve of the glucose tolerance test and food and liquid consumptions, where two-way ANOVA were performed. Comparisons were followed by the Bonferroni's *post-hoc* test for multiple comparisons. Significance was defined as $p < 0.05$.

3. Results

3.1. Characterisation of 3xTg-AD and NonTg mice under chronic hyperglycaemia

To characterise the metabolism of the sucrose-treated 3xTg-AD and NonTg mice animals were weighed and their liquid and ration intakes monitored over 6 months (from 2 to 8 months of age). Glucose tolerance tests were performed at baseline. At the end of treatment, glucose tolerance tests were also performed as well as random glucose tests and postprandial glycaemia measurements. Metabolic characterization was also performed in the respective untreated mice.

Glucose metabolism. No differences were found between animal groups regarding random or postprandial glycaemia at the end of treatment (Figs. 1A and 1B) nor between groups at the baseline glucose tolerance test (data not shown). As regard to the glucose tolerance test performed at end of treatment (Fig. 1C), the 3xTg-AD-8C group achieved the lowest glycaemias at every timepoint apart from $t = 0$. That said, the sucrose-fed groups achieved the highest glycaemias for these timepoints, the NonTg-8Suc prevailing between $t =$ 30 min and $t = 60$ min and the 3xTg-AD-8Suc being dominant from $t = 90$ min to the end of the test. Peak glycaemias were achieved by all groups at $t = 30$ min. In the case of the sucrose-fed, glycaemia assessment was limited by the maximum range (6g/L) of the measurement instrument. The 3xTg-AD-8Suc mice had significantly higher glycaemias from their control transgenic counterparts in every timepoint apart fom $t = 90$ (repeated measures two-way ANOVA; $p < 0.001$ for $t = 0$, $t = 30$ min and $t = 60$ min; $p < 0.05$ for $t = 15$ min and $t = 120$ min). The NonTg-8C had significantly higher glycaemias than the 3xTg-AD-8C at timepoints $t = 30$ min (repeated measures two-way ANOVA; $p < 0.05$) and $t = 60$ min (repeated measures two-way ANOVA; $p < 0.001$). Accordingly, sucrose treatment had areas under the curve (AUCs) for glucose concentrations during the glucose tolerant test

significantly higher than their NonTg counterparts (two-way ANOVA; $F_{(1,18)} = 54.99$; $p < 0.001$; Fig 1D). There is a trend for significance concerning the effects of 3xTg-AD genotype (two-way ANOVA; $F_{(1,18)} = 4.407$; $p = 0.0502$) and of the interaction between the 3xTg-AD genotype and sucrose treatment (two-way ANOVA; $F_{(1,18)} = 4.263$; $p = 0.0537$). The 3xTg-AD-8Suc had a glycaemia AUC significantly higher than the 3xTg-8C (two-way ANOVA; $p < 0.001$) and from the NonTg-8C (two-way ANOVA; $p = 0.0052$). Moreover, the NonTg-8Suc also showed an AUC significantly higher (two-way ANOVA; $p < 0.001$) than the 3xTg-AD-8C. Finally, the NonTg-8Suc achieved significantly greater AUC than their control (two-way ANOVA; $p = 0.0049$); the NonTg-8Suc presented greater AUC mean values (50387.5 ± 4596.7) than the 3xTg-AD-8C (24915 ± 3073.9), although diferences were not significant (two-way ANOVA; $p = 0.0721$).

Mice weight. The 3xTg-AD-8Suc had a significantly greater overall weight increase from the baseline than the NonTg-Suc and the NonTg-8C (Fig. 1E) (repeated measures two-way ANOVA; $p < 0.01$). In terms of percentual weight gain, 3xTg-AD-8Suc and, to a lesser extent, NonTg-8Suc thrived the most (177.6% ± 30.2 and 166% ± 41.3 from the starting weight, respectively), while the 3xTg-AD-8C showed a blunted growth, having achieved the least percentual gain (130% ± 12.4 of the starting weight) (Fig. 1F). Glucose treatment yielded significantly higher percentual weight gains (repeated measures two-way ANOVA; $F = 6.228$; $p < 0.05$). The 3xTg-AD-8Suc had significantly higher percentual weight gains than the 3xTg-AD-8C (repeated measures two-way ANOVA; $p < 0.05$) in the latter months of treatment. The NonTg-8Suc also had higher percentual gains than their control at various timepoints (repeated measures two-way ANOVA; $p < 0.05$).

Liquid intakes. Liquid intakes were significantly higher in the sucrose-fed (two-way ANOVA; $F_{(1,18)} = 34.86$; $p < 0.001$) and in the transgenic groups (two-way ANOVA; $F_{(3,18)} = 145.2$; $p < 0.001$, relatively untreated mice (Fig. 1G). Nevertheless, there was no statistically

significant interaction between genotype and sucrose treatment in liquid intake. The 3xTg-AD-8Suc had significantly higher liquid intakes than the 3xTg-AD-8C and NonTg-8C (two-way ANOVA; $p < 0.001$) and the NonTg-8Suc (two-way ANOVA; $p < 0.05$). The 3xTg-AD-8C had significantly higher intakes than the NonTg-8C (two-way ANOVA; $p < 0.05$), but lesser than the NonTg-8Suc (two-way ANOVA; $p < 0.05$). Lastly, the NonTg-8Suc had significantly higher consumptions than their control (two-way ANOVA; $p < 0.001$).

Food consumption. Results concerning the effect of genotype and sucrose treatment (Fig. 1H) also attained significance for both genotype (two-way ANOVA; $F_{(1,18)} = 126.8$; $p < 0.001$) and sucrose treatment (two-way ANOVA; $F_{(1,18)} = 26.45$; $p < 0.001$), but not for the interaction thereof. The 3xTg-AD-8Suc had significantly lesser intakes than the 3xTg-AD-8C (two-way ANOVA; $p < 0.001$) and the NonTg-8C (two-way ANOVA; $p < 0.01$), but not relatively to the NonTg-8Suc. The 3xTg-AD-8C showed significantly greater intakes than the sucrose-treated and untreated NonTg mice (two-way ANOVA; $p < 0.01$ and $p < 0.001$ respectively). The NonTg-8C had significantly greater intakes than its sucrose-fed counterpart (two-way ANOVA; $p < 0.001$).

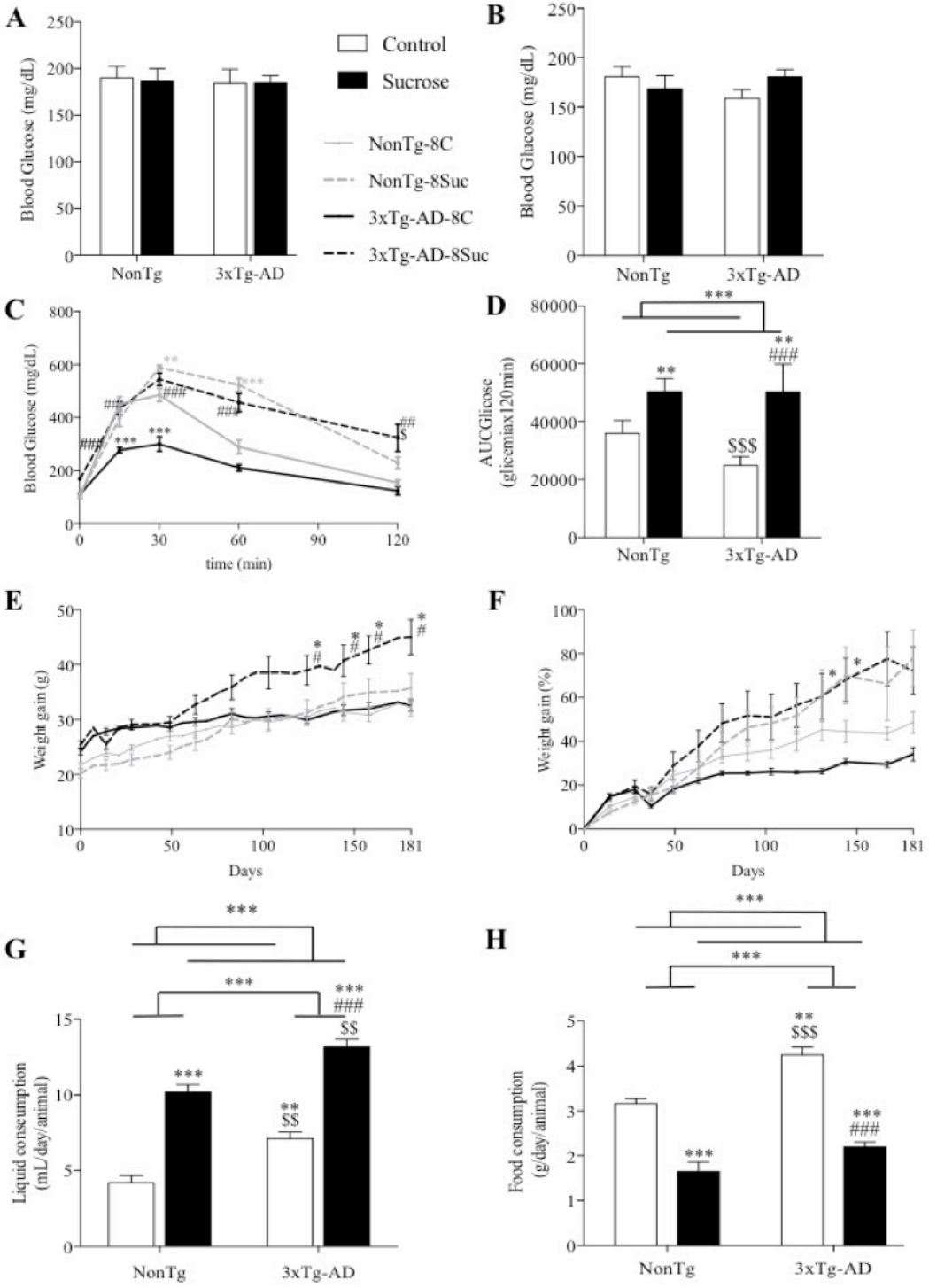

Figure 1. Metabolic characterisation of 8 month-old NonTg and 3xTg-AD mice after 6 months of sucrose treatment. (**A**) random glucose test. (**B**) postprandial glycaemia measurement. (**C**) intraperitoneal glucose tolerance test and area (**D**) under the two-hour blood glucose response curve. Sucrose treament by itself lessens glucose tolerance ($p < 0.001$). Glucose tolerance is decreased in NonTg-8Suc, 3xTg-AD-8C and 3xTg-AD-8Suc. (**E**) Weight gain starting from the age of 2 months. Weight is increased in 3xTg-AD-8Suc. (**F**) Percentual weight gain starting from the age of 2 months. Average liquid (**G**) and food (**H**) consumptions. Sucrose treatment induces increase in liquid consumption and decrease in food consumption ($p < 0.001$). 3xTg-AD genotype induces an increase in liquid and food consumption ($p < 0.001$). Data are expressed as mean ± SEM for 4-6 animals per group. Statistical analysis: *$p < 0.05$, ,**$p < 0.01$, ***$p < 0.001$ vs NonTg; \$$p < 0.05$, \$\$$p < 0.01$, \$\$\$$p < 0.001$ vs NonTgSuc; #$p < 0.05$, ##$p < 0.01$, ###$p < 0.001$ vs 3xTg-AD (two-way ANOVA followed by Bonferroni post-hoc test (A, B, D, G, H); repeated measures two-way ANOVA followed by Bonferroni *post hoc* test (C, E, F).

3.2. Age-related β-catenin levels in hippocampal neuroblasts and immature neurons

β-catenin integrated density per area (IDA) measurements were carried out for the nucleus, cytosol and processes or dendrites of neuroblasts, immature neurons and mature neurons, as shown in figure 2. The 3xTg-AD-2mo. show significantly higher IDAs than the NonTg-2mo. for the threshold range in the cytosol of neuroblasts (repeated measures two-way ANOVA; $p < 0.01$) and in the dendrites of immature neurons for thresholds 12-15 (repeated measures two-way ANOVA; $p < 0.01$ for thresholds 12-13; $p < 0.001$ for thresholds 14-15). Also, the 3xTg-AD-2mo. have significantly higher IDAs in comparison with the 3xTg-AD-8mo. in the dendrites of immature neurons throughout the range of thresholds (repeated measures two-way ANOVA; $p < 0.05$ for thresholds 0-11; $p < 0.01$ for thresholds 12-15). No other statistical differences were found between groups of either genotype or age (2-month-old *vs*. 8-month-old) for any of the cells and cellular constituents analysed. A trend to increased nuclear and cytosolic β-catenin IDA in the 3xTg-AD-2mo.group can be observed in immature neurons. Lastly, β-catenin IDAs appear to be smaller in mature neurons for each cellular location, in comparison to either neuroblasts or immature neurons and irrespective of animal age.

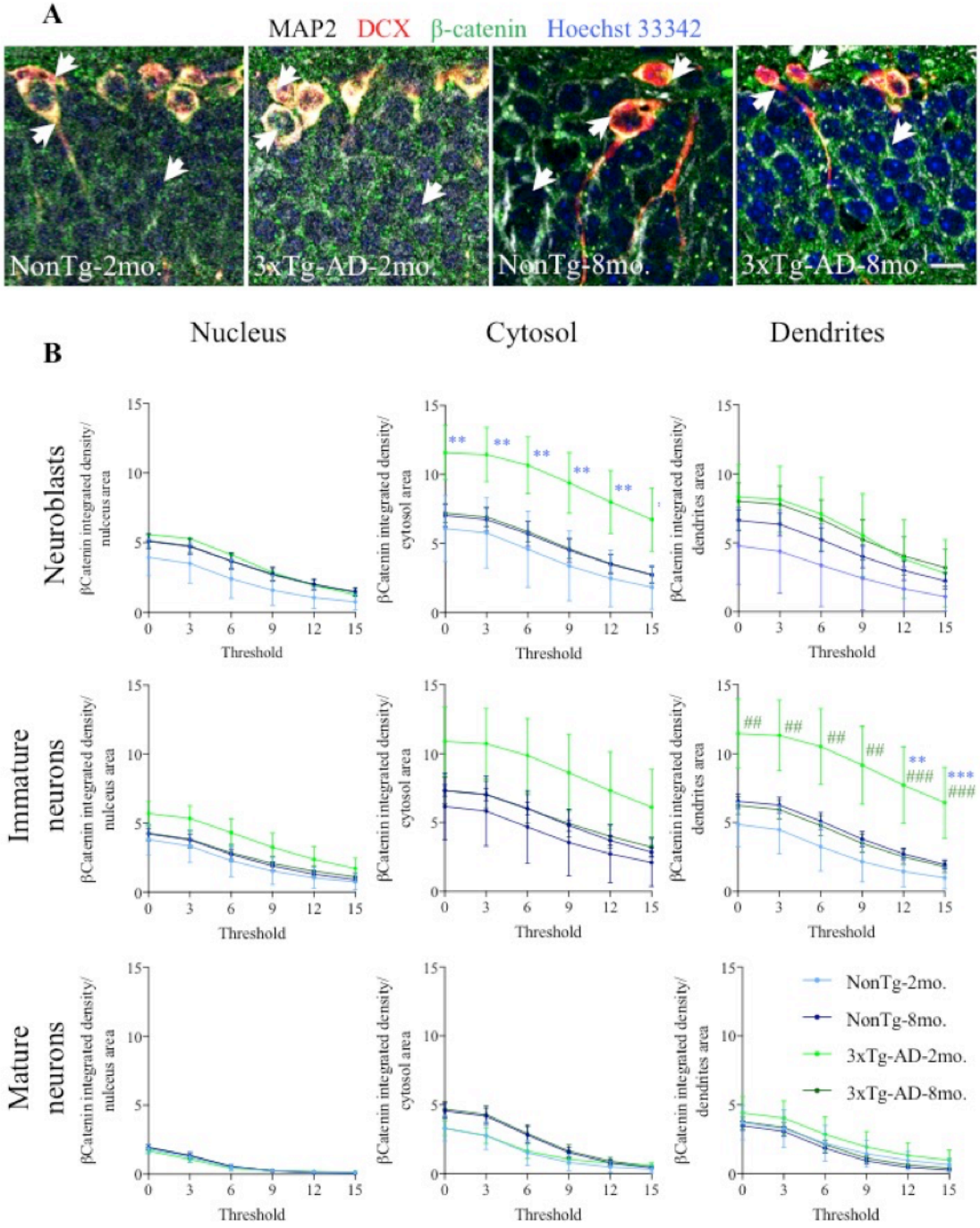

Figure 2. (**A**) Representative images of neuroblasts, immature and mature neurons (signalled with arrow heads) of NonTg-2mo., NonTg-8mo., 3xTg-AD-2mo. and 3xTg-AD-8mo. mice in the granular cell layer of the dentate gyrus were obtained through single-plane confocal microscopy, as described in Materials and methods. Staining was performed with anti-MAP2, anti-DCX and anti-β-catenin specific antibodies, and hoechst 33342. Scale: 10 µm. (**B**) β-Catenin integrated density per area in the nuclei, cytosol and dendrites of neuroblasts, immature and mature neurons of NonTg-2mo., NonTg-8mo., 3xTg-AD-2mo. and 3xTg-AD-8mo. mice. 3xTg-AD-2mo. neuroblasts display significantly higher cytosolic integrated densities per area than NonTg-2mo.. 3xTg-AD-2mo. immature neurons have significantly higher dendritic integrated densities per area than NonTg-2mo. and than 3xTg-AD-8mo.. Data are expressed as mean ± SEM for 2-7 3xTg-AD animals/group (2 or 8 months, respectively) and 2-7 NonTg animals/group (2 or 8 months, respectively). Statistical analysis: $^{**}p < 0.01$, $^{***}p < 0.001$ *vs* NonTg-8mo.; $\#\#p < 0.01$, $\#\#\#p < 0.001$ *vs* 3xTg-AD-8mo. (repeated measures two-way ANOVA followed by Bonferroni *post hoc* test).

The ratios between the total integrated densities of β-catenin of nucleus and cytoplasm were calculated for each threshold for NonTg and 3xTg-AD animals of either age (Fig. 3).

The neuroblasts in 3xTg-AD-2mo. have significantly lesser ratios relative to 3xTg-AD-8mo. throughout the threshold range (repeated measures two-way ANOVA; $p < 0.001$) and NonTg-8mo. (repeated measures two-way ANOVA; $p < 0.05$) for thresholds 0 to 4. Furthermore, the NonTg-2mo. neuroblasts also had lesser nuclear translocation than its 8-month-old counterpart for thresholds 6 to 15. Lastly, the 3xTg-AD-2mo. immature neurons have significantly lesser ratios than 3xTg-AD-8mo. for thresholds 0 to 12 and than NonTg-8mo. for thresholds 0 to 3. For these cells, age had a statistically significant effect (repeated measures two-way ANOVA; $F = 6.185$; $p < 0.05$).

To summarise, these findings point to an accumulation in the cytosol of β-catenin in the neuroblasts and immature neurons of 3xTg-AD 2 month-old mice, when compared with 8 month-old animals of either genotype. The immature neurons of non-transgenic 2 month-old animals have a similar pattern as regards to their 8 month-old counterpart.

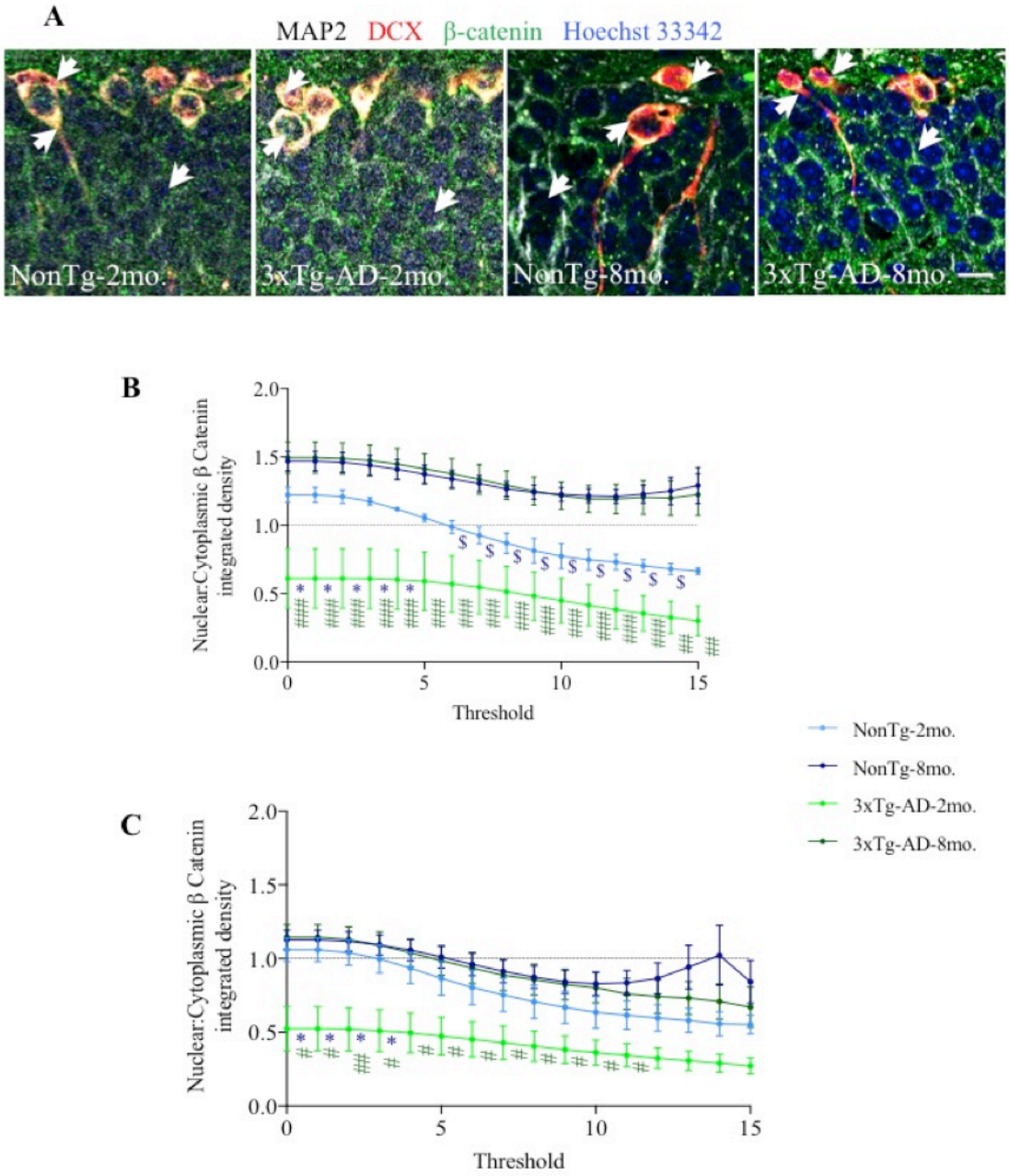

Figure 3. (**A**) Representative images of neuroblasts, immature and mature neurons (signalled with arrow heads) of NonTg-2mo., NonTg-8mo., 3xTg-AD-2mo. and 3xTg-AD-8mo. mice in the granular cell layer of the dentate gyrus were obtained through single-plane confocal microscopy, as described in Materials and methods. Staining was obtained with anti-MAP2, anti-DCX and anti-β-catenin specific antibodies, and hoechst 33342. Scale 10 µm. Nuclear and cytosolic ratio of β-Catenin integrated density of neuroblasts (**B**) and immature neurons (**C**) of NonTg-2mo., NonTg-8mo., 3xTg-AD-2mo. and 3xTg-AD-8mo. mice. Neuroblasts from 3xTg-AD-2mo. have significantly lower nuclear and cytosolic ratio than 3xTg-AD-8mo. and than NonTg-8mo.. NonTg-2mo. neuroblasts have significantly lower nuclear and cytosolic ratio than NonTg-8mo.. 3xTg-AD-2mo. immature neurons have significantly lower nuclear and cytosolic ratio than 3xTg-AD-8mo. and than NonTg-8mo. Data are expressed as mean ± SEM for 2-7 3xTg-AD animals/group (2 or 8 months, respectively) and 2-7 NonTg animals/group (2 or 8 months, respectively). Statistical analysis: *$p < 0.05$ *vs* NonTg-2mo; \$$p < 0.05$ *vs* NonTg-8mo; #$p < 0.05$, ##$p < 0.01$, ###$p < 0.001$ *vs* 3xTg-AD-8mo (repeated measures two-way ANOVA followed by Bonferroni *post hoc* test).

3.3. Hyperlgycemia-induced changes in β-catenin subcellular distribution in hippocampal immature neurons from 3xTg-AD mice

The analysis of β-catenin integrated density per area measurements was identical as the one mentioned in the previous subsection and was performed for each of the groups of the 8-month-old animals. No statistical differences were found between groups regarding β-catenin levels in neuroblasts, immature neurons and mature neurons for the respective nuclei, cytosol, or processes or dendrites (Fig. 4).

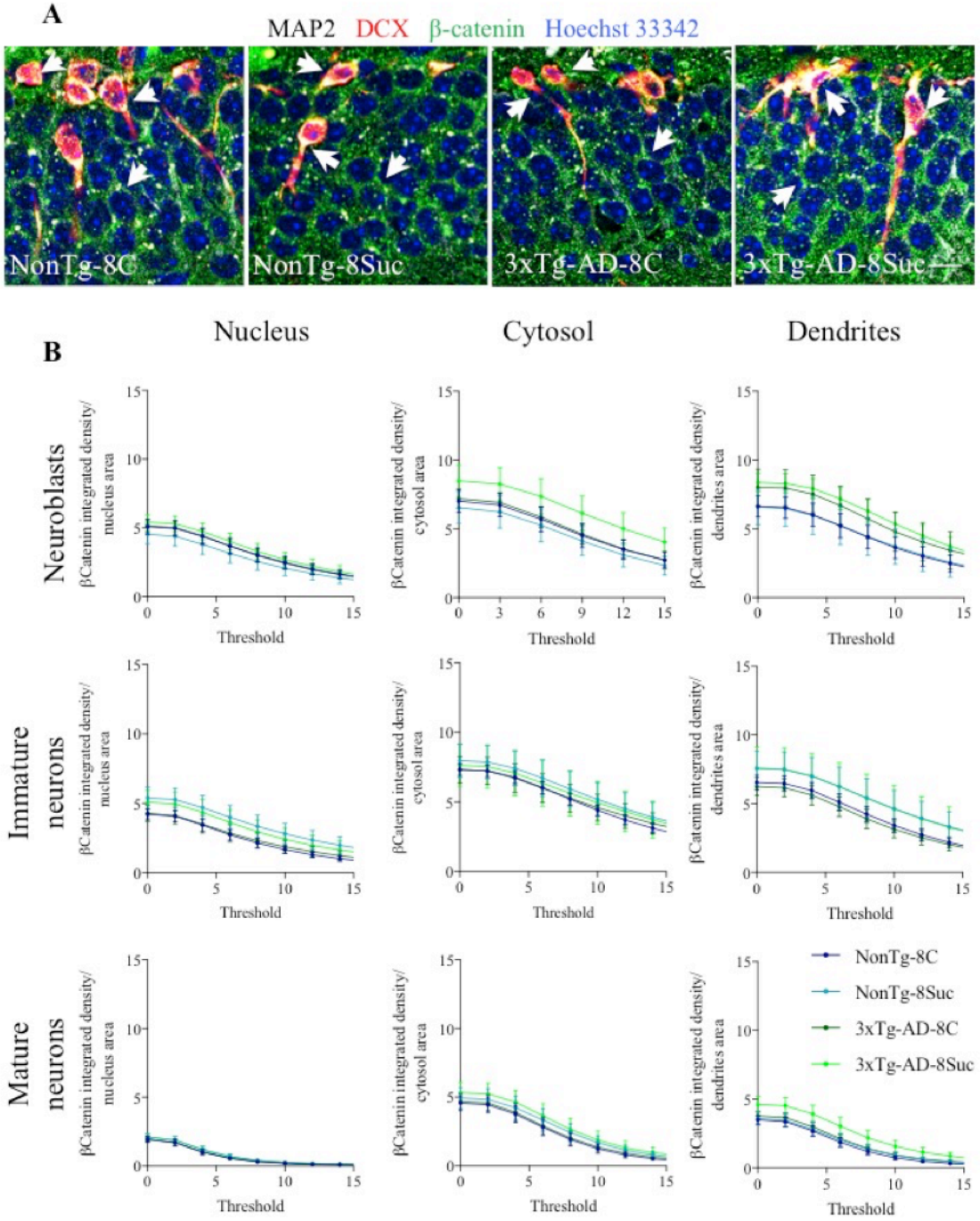

Figure 4. (**A**) Representative images of neuroblasts, immature and mature neurons of NonTg-8C, NonTg-8Suc, 3xTg-AD-8C and 3xTg-AD-8Suc mice (signalled with arrow heads) in the granular cell layer of the dentate gyrus were obtained through single-plane confocal microscopy, as described in Materials and methods. Staining was performed with anti-MAP2, anti-DCX and anti-β-catenin specific antibodies, and hoechst 33342. Scale 10 μm. (**B**) β-Catenin integrated density per area in the nuclei, cytosol and dendrites of neuroblasts, immature and mature neurons of NonTg-8C, NonTg-8Suc, 3xTg-AD-8C and 3xTg-AD-8Suc mice. No statistical differences were found between groups. Data are expressed as mean ± SEM for 7 animals/group. Statistical analysis: repeated measures two-way ANOVA followed by Bonferroni *post hoc* test.

The cellular localization of β-catenin and its accumulation in the nucleus was evaluated by the calculation of the ratios of total integrated densities of β-catenin between the nucleus and cytosol, for each threshold, for untreated and sucrose-treated 8 month-old NonTg and 3xTg-AD mice (Fig. 5). There were no significative differences between the groups in the total IDA ratios of the neuroblasts. In what concerns the immature neurons, the 3xTg-AD-8Suc showed significantly greater ratios than the 3xTg-AD-8C throughout the near entirity of the threshold range (repeated measures two-way ANOVA; $p < 0.05$) (Fig. 5C). This points to a nuclear accumulation of β-catenin specific of the immature neurons of sucrose-treated transgenic mice when they are compared with the non-treated transgenic animals.

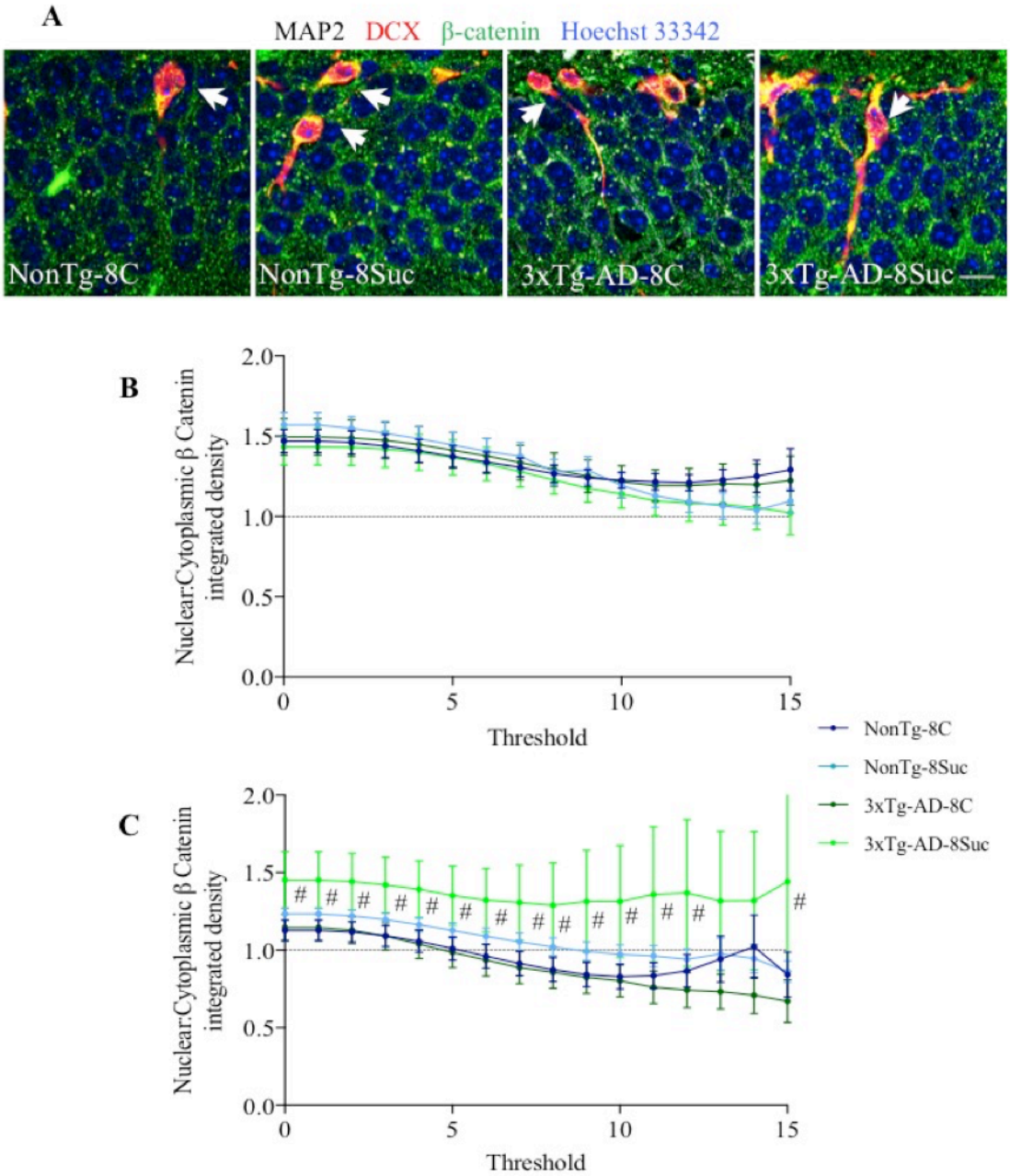

Figure 5. (**A**) Representative images of neuroblasts, immature and mature neurons of NonTg-8C, NonTg-8Suc, 3xTg-AD-8C and 3xTg-AD-8Suc mice (signalled with arrow heads) in the granular cell layer of the dentate gyrus were obtained through single-plane confocal microscopy, as described in Materials and methods. Staining was performed with anti-MAP2, anti-DCX and anti-β-catenin specific antibodies, and hoechst 33342. Scale 10 µm. Nuclear to cytosolic ratio of β-catenin integrated density of neuroblasts (**B**) and immature neurons (**C**) of NonTg-8C, NonTg-8Suc, 3xTg-AD-8C and 3xTg-AD-8Suc mice. 3xTg-AD-8Suc immature neurons have significantly higher nuclear to cytosolic ratios than 3xTg-AD-8C. Data are expressed as mean ± SEM for 8 or 5 3xTg-AD animals/group (untreated or sucrose-treated, respectively) and 7-8 NonTg animals/group (untreated or sucrose-treated, respectively). Statistical analysis: #$p < 0.05$ (repeated measures two-way ANOVA followed by Bonferroni *post hoc* test).

4. Discussion

Dysfunction of Wnt/β-catenin pathway in AD has been established in the literature. Because of its pivotal role in adult hippocampal neurogenesis, it is believed that alterations in this pathway negatively impact this process. In this work, this concept was integrated in the context of a diabetes-like state.

A putative exacerbation of the affection of the Wnt/β-catenin was explored through the use of a transgenic murine model of AD, with known AD-like neuropathological phenotype, under chronic hyperglycaemia. Full characterisation of the 3xTg-AD mice metabolic profile exceeds the aim of this study and was previously reported [24,26-30]. The data gathered on the metabolism of the mice groups are in accordance with a diabetes-like syndrome. Having gathered these conditions, β-catenin levels and distribution were assessed in different cells of the granule cell layer of the dentate gyrus, namely neuroblasts and immature and mature neurons, with respect to their nuclei, cytosol and cellular processes (in neuroblasts) or dendrites (in the later phenotype). Age-related changes in the levels of β-catenin were also explored by comparing 2 and 8 months of age 3xTg-AD and control animals.

β-catenin is a versatile protein that integrates a myriad of functions in different cellular locations, including the nucleus, cytosol and cellular membranes [31]. For this reason, its regulation is dependent on multiple interplaying factors. The major factor in β-catenin activity regulation is its proteasomal degradation in the cytoplasm, which occurs continuously [32,33]. In physiologic states of Wnt pathway activation, β-catenin accumulation occurs and displays a predominantly cytoplasmic distribution pattern in the form of granules [34,35]. This concurs with the data which are presented herein, considering that β-catenin density appears to be higher in the cytosol in comparison to that found in the nucleus of neuroblasts

and immature and mature neurons of both 2- and 8-month-old NonTg mice. In the case of young 3xTg-AD mice, this cytosolic distribution is enhanced when compared to both NonTg and 8-month-old 3xTg-AD mice. This could be consequential to early proteasome dysfunction in the context of an incipient decline in the precursor lineage of hippocampal neurons. In addition, unpublished data obtained by our group revealed that, with ageing, a progressive decline in the numbers of neuroblasts and newly generated neurons occurs. In this cenario, an increase of β-catenin levels in the nucleus would serve as a mechanism oto promote cellular survival, proliferation and differentiation, in an attempt to counterbalance depletion of these cells. This rationale corroborates the data described above where both neuroblasts and immature neurons of 8 month-old 3xTg-AD mice have a higher ratio of nuclear to cytosol total β-catenin levels when compared to younger 3xTg-AD mice, despite the absence of differences relatively to the NonTg animals.

The comparison and contrast between younger and older animals of both genotypes in the former experiment allowed for the interpretation of the findings concerning the treatment with sucrose in a more robust context. As regards the results from the sucrose treatment, the ratio between nuclear and cytosolic β-catenin levels is, in newly generated neurons, significantly greater in 3xTg-AD-8Suc relative to 3xTg-AD-8C. This could be explained by β-catenin translocation to the nucleus, which could be integrated as a compensatory response involving the canonical Wnt/β-catenin pathway to sustain cellular stress derived from AD pathology [9,10,36] and the effects of chronic hyperglycaemia [36,37]. Unpublished work from our group shows that in 3xTg-AD animals, and more so in the sucrose-fed group, the precursor cell population is scarcer, and that there is a decrease in the complexity and differentiation of the immature neurons when compared to NonTg mice. Inhibition of β-catenin signalling has been associated with augmented apoptosis in hippocampal neurons [34,38,39]. For these reasons, it is possible that increased levels of nuclear β-catenin, perhaps

secondary to increased translocation and/or retention in the nucleus by interacting factors, aim to promote precursor survival and stimulate compensatory hyperplasia [40-42] in the animal with hindered hippocampal precursor reserve, in an analogous fashion to what happens upon depletion of pancreatic islet β-cells in prediabetic mice [43]. Further corroborating this hypothesis, the canonical Wnt/β-catenin pathway has a protective role against Aβ [44] and impacts the extent and morphology of dendritic arborization [4,22]. Upon pathologic exposure to Aβ [45], Wnt pathway dysfunction, brought about by increased GSK-3β activity [4,19,20] was shown to preclude cytosolic β-catenin accumulation in a dose-dependent manner in hippocampal neurons [45]. In primary neurons, increased expression of wild type and mutant amyloid precursor protein altered the distribution pattern of β-catenin according to its subcellular location, namely affecting the cytosolic β-catenin levels and being innocuous in the nucleus, without disturbing β-catenin's activity as a transcription factor [46]. In the setting of chronic hyperglycaemia, production of Aβ and its more neurotoxic byproduct Aβ-AGE occurs at a faster rate [10]. Both forms, but in particular the latter, act as inhibitors of Wnt/β-catenin signalling through GSK-3β signalling [4,10,47] and may ultimately lead to augmented apoptosis in neuroblasts and immature neurons of 3xTg-AD-8Suc, thus possibly explaining the scarcity of cells in these stages of maturation. The enhanced dysfunction of Wnt signalling and consequential cytosolic β-catenin degradation also supports the rationale behind the significantly higher nuclear/cytosolic β-catenin levels in 3xTg-AD-8Suc relatively to 3xTg-AD-8C. Experiments showing increased phosphorylated β-catenin in the cytosol (an indicator of β-catenin disposal) [46,48] further corroborated the hypothesis that the apparent nuclear translocation of β-catenin could be a pseudo-redistribution secondary to enhanced cytoplasmic degradation, whilst its nuclear levels remained relatively unnafected [46]. Furthermore, dysfunction of the Wnt pathway has been shown to lack impact in nuclear translocation [32], which could favour the hypothesis that there is selective degradation of β-

catenin in the cytosol and this is the main factor controlling β-catenin distribution. Nevertheless, proteasome inhibition by Aβ has been documented in 3xTg-AD mice [48,49] and the effects of that inhibition on the levels of β-catenin are, to a large extent, unpredictable and should be integrated in future investigations. Lastly, many of the referenced studies were performed on mature hippocampal neurons or primary cultures. Extrapolation of these findings to immature neurons and neuroblasts is not without risk of oversimplification.

Another intervening mechanism is the nuclear import and export of β-catenin, which is dependent on the properties and constituents of the nuclear envelope [32,35]. Despite being a 90 kDa protein, translocation of β-catenin through the pores of the nuclear envelope is an efficient process (with equilibration occurring within 10 minutes) [32]. However, this translocation process is, to some extent, dependent of and enhanced by import and export machineries. Furthermore, it is dependent on the binding of β-catenin with its nuclear (e.g., transcription factor 4 (TCF4), B-cell CLL/lymphoma 9 (BCL9)) and cytosolic (e.g., adenomatous poliposis coli (APC), axin, axin2/conduction) interaction partners, which act as determinants of β-catenin location through promotion of its retention in their respective subcellular compartment [32]. Subsequent lines of investigation could be aimed at evaluating the activity and co-localization of β-catenin's interaction partners and their influence in determining selectivity of the molecule to the nucleus in AD-like states, if possible, under the influence of diabetic phenotype.

Lastly, the nucleus may act as a reservoir for β-catenin in pathological states, whose function would be to prevent β-catenin depletion when its accumulation is impaired. Another possibility is that, in face of β-catenin depletion, the need for nuclear β-catenin, namely for its function as a transcription factor, is dominant relatively to other subcellular compartments.

Taking into account the results obtained in this work, we argue that age-related β-catenin redistribution to the nucleus could represent an attempt to compensate for depletion of

immature neurons and decreased maturation derived from the cumulative effects of AD and chronic hyperglycaemia. β-catenin would tend to promote cell survival and hyperplasia with the ultimate goal of replenishing the precursor lineage and compensate for losses. On the other hand, increasing rates of cytosolic degradation of β-catenin with age could also explain these results.

5. Conclusion

This study innovatively approached the analysis of β-catenin levels and its subcellular distribution in the precursor lineage of the hippocampal neurons. We found evidence of redistribution of cellular β-catenin to the nucleus along age and under the influence of AD pathology and a diabetes-*like* phenotype in this population of cells. We have also identified areas of future investigation, which could aid in deciphering the mechanisms underlying the preferential distribution of β-catenin under the effects of ageing, AD pathology and a diabetes-*like* syndrome.

6. Funding and disclosure of competing interest

The authors gratefully acknowledge the funding by the 'Programa Operacional Temático Factores de Competividade 2020, COMPETE_2020', the European community fund FEDER, and the 'Fundação para Ciência e a Tecnologia' (FCT) UID/NEU/04539/2013.

This work was supported by the Research Support Office (‘Gabinete de Apoio à Investigação’, GAI) funded by the Faculty of Medicine of the University of Coimbra and Santander Totta Bank, project reference FMUC-BST-2016/205.

The authors declare no conflict of interest.

7. Acknowledgements

I would like to express my gratitude to Professor Cristina Rego for welcoming me into the Mitochondrial Dysfunction and Signalling in Neurodegeneration research group and for providing me with the opportunity and guidance to pursue this endeavour. I am most appreciative of her patience and understanding during this year.

I am deeply endebted to Dr. Elisabete Ferreiro, whose diligence and tireless support allowed this work to come to fruition. I am appreciative of her guidance and teachings of perseverance and care for detail.

I thank Dr. Jorge Valero's invaluable contribution to the design of the macros that paved the way to the collection of long-desired data.

My gratitude to Professor Paulo Pinheiro for the help with the use of the vibratome and to Dr. Margarida Caldeira for her help with the confocal microscope.

I am grateful to all the researchers of the group for welcoming me and for their willingness to help throughout the entirety of my stay in the laboratory.

To my fellow students of the group, thank you for your companionship in the laboratory.

I would also like to express my gratitude to the staff of the Centre's animal house for all their assistance.

Lastly, I gratefully acknowledge the opportunity of having written this dissertation in the Centre for Neuroscience and Cell Biology.

To my parents, who keep me grounded whilst inspiring me to go above and beyond.

8. References

1. Alzheimer's Disease International. World Alzheimer Report [document on the Internet]. London: Alzheimer's Disease International; 2015 [updated 2015 October, cited 28 August 2015]. Available from: https://www.alz.co.uk/research/world-report-2015.

2. Richards SS, Hendrie HC. Diagnosis, management, and treatment of Alzheimer disease: a guide for the internist. Arch Intern Med. 1999;159(8):789-98.

3. Serrano-Pozo A, Frosch MP, Mashliah E, Hyman BT. Neuropathological alterations in Alzheimer disease. Cold Spring Harb Perspect Med. 2011;1(1):a006189

4. Wan W, Xia S, Kalionis B, Liu L, Li Y. The role of Wnt signaling in the development of Alzheimer's disease: a potential therapeutic target? Biomed Res Int [document on the Internet]. 2014 May [cited 2015 Nov 10]; 2014:301575:[about 9pp.]. Available from: http://dx.doi.org/10.1155/2014/301575.

5. Sims-Robinson C, Kim Bhumsoo, Rosko A, Feldman EL. How does diabetes accelerate Alzheimer disease pathology? Nature Reviews Neurology. 2010;6(10):551-9.

6. Watson GS, Craft S. The role of insulin resistance in the pathogenesis of Alzheimer's disease: implications for treatment. CNS Drugs. 2003;17(1):27-45.

7. Neumann KF, Rojo L, Navarrete LP, Farias G, Reyes P, Maccioni RB. Insulin resistance and Alzheimer's disease: molecular links & clinical implications. Curr Alzheimer Res. 2008;5(5):438-47.

8. de la Monte SM., Wands JR. Alzheimer's disease is type 3 diabetes - Evidence revisited. J Diabetes Sci Technol. 2008;2(6):1101-13.

9. Barbagallo M, Dominguez LJ. Type 2 diabetes and Alzheimer's disease. World J Diabetes. 2014;15(6):889-893.

10. Li XH, Du LL, Cheng XS, Jiang X, Zhang Y, Lv BL et al. Glycation exacerbates the neuronal toxicity of β-amyloid. Cell Death Dis [document on the Internet]. 2013 Jun [cited 2015 Nov 10]; 4(6):e673:[about 9pp.]. Available from: http://www.nature.com/cddis/journal/v4/n6/pdf/cddis2013180a.pdf.

11. Taupin P. Adult neural stem cells, neurogenic niches, and cellular therapy. Stem Cell Rev. 2006;2(3):213-9.

12. Ehninger D, Kempermann G. Neurogenesis in the adult hippocampus. Cell Tissue Res. 2008;331(1):243-50.

13. Piatti VC, Ewell LA, Leutgeb JK. Neurogenesis in the dentate gyrus: carrying the message or dictating the tone. Front Neurosci. 2013;7(50):1-11.

14. Ottone C, Parrinello S. Multifaceted control of adult SVZ neurogenesis by the vascular niche. Cell Cycle. 2015;14(14):2222-5.

15. Schmidt B, Marrone DF, Markus EJ. Disambiguating the similar: the dentate gyrus and pattern separation. Behavioural Brain Research. 2012;226(1):56-65.

16. Kempermann G, Song H, Gage FH. Neurogenesis in the adult hippocampus. Cold Spring Harb Perspect Biol. 2015;7(9):a018812.

17. Mu Y, Gage FH. Adult hippocampal neurogenesis and its role in Alzheimer's disease. Mol Neurodegener. 2011;6(85):1-9.

18. Inestrosa NC, Varela-Nallar L. Wnt signaling in the nervous system and in Alzheimer's disease. J Mol Cell Biol. 2014; 5(1):64-74.

19. Hooper C, Killick R, Lovestone S. The GSK3 hypothesis of Alzheimer's disease. J neurochem. 2008;104(6):1433-9.

20. Hur EM, Zhou FQ. GSK signalling in neural development. Nat Rev Neurosci. 2010;11(8):539-51.

21. Lie DC, Colamarino SA, Song HJ, Désiré L, Mira H, Consiglio A, et al. Wnt signalling regulated adult hippocampal neurogenesis. Nature. 2005;437(7063):1370-5.

22. Gao X, Arlotta P, Macklis JD, Chen J. Conditional knock-out of beta-catenin in postnatal-born dentate gyrus granule neurons results in dendritic malformation. J Neurosci. 2007;27(52):14317-25.

23. Oddo S, Caccamo A, Sheperd JD, Murphy MP, Golde TE, Kayed R. Triple-transgenic model of Alzheimer's disease with plaques and tangles: intracellular Aβ and synaptic dysfunction. Neuron. 2003;39(3):409-21.

24. Mota SI, Ferreira IL, Valero J, Ferreiro E, Carvalho AL, Oliveira CR, et al. Impared Src signaling and post-synaptic actin polymerization in Alzheimer's disease mice hippocampus - Linking NMDA receptors and the reelin pathway. Exp. Neurol. 2014;261:698-709

25. Schindelin J, Arganda-Carreras I, Frise E, Kaynig V, Longair M, Pietzsch T. Fiji: an open-source platform for biological-image analysis. Nat Methods. 2012;9(7):676-82.

26. Carvalho C, Cardoso S, Correia SC, Santos RX, Santos MS, Baldeiras I, et al. Metabolic alterations induced by sucrose intake and Alzheimer's disease promote similar brain mitochondrial abnormalities. Diabetes. 2012;61(5):1234-42.

27. Vandal M, St-Amour I, Marette A, Calon F. Age-dependent impairment of glucose tolerance in the 3xTg-AD mouse model of Alzheimer's disease. FASEB J. 29(10):4273-84.

28. Knight EM, Verkhratsky A, Luckman SM, Allan SM, Lawrence CB. Hypermetabolism in a triple-transgenic mouse model of Alzheimer's disease. Neurobiol Aging. 2012;33(1):187-93.

29. Adebakin A, Bradley J, Gümüsgöz S, Waters EJ, Lawrence CB. Impaired satiation and increased feeding behaviour in the triple-transgenic Alzheimer's disease mouse model. PLoS One. 2012;7(10):e45179. doi: 10.1371/journal.pone.0045179.

30. Dias C, Lourenço CF, Ferreiro E, Barbosa RM, Laranjinha J, Ledo A. Age-dependent changes in the glutamate-nitric oxide pathway in the hippocampus of the triple transgenic model of Alzheimer's disease: implications for neurometabolic regulation. Neurobiol Aging. 2016;46:84-95.

31. Wisniewska. Physiological role of β-Catenin/TCF signaling in neurons of the adult brain. Neurochem Res. 2013;38(6):1144-1155.

32. Krieghoff E, Behrens J, Mayr B. Nucleo-cytoplasmic distribution of beta-catenin is regulated by retention. J Cell Sci. 2006.119(Pt. 7):1453-63.

33. Aberle H, Bauer A, Stappert J, Kispert A, Kemler R. β-Catenin is a target for the ubiquitin-proteasome pathway. EMBO J. 1997;16(13):3797-804.

34. Zhang Z, Hartmann H, Do VM, Abramowski D, Sturchler-Pierrat C, Staufenbiel M, et al. Destabilization of beta-catenin by mutations in presenilin-1 potentiates neuronal apoptosis. Nature. 1998.395(6703):698-702.

35. Maturana JL, Niechi I, Silva E, Huerta H, Cataldo R, Härtel S. Transactivation activity and nucleocytoplasmic transport of β-catenin are independently regulated by its C-terminal end. Gene. 2015;573(1):115-22.

36. Balu DT, Lucki I. Adult hippocampal neurogenesis: regulation, functional implications, and contribution to disease pathology. Neurosci Biobehav Rev. 2009;33(3):232-52.

37. Zhang WJ, Tan YF, Yue JT, Vranic M, Wojtowicz JM. Impairment of hippocampal neurogenesis in streptozotocin-treated diabetic rats. Acta Neuro Scand. 2008;117(3):205-10.

38. Pereira C, Ferreiro E, Cardoso SM, Oliveira CR. Cell degeneration induced by amyloid-beta peptides: implications for Alzheimer's disease. J Mol Neurosci. 2004;23(1-2):97-104.

39. Mota SI, Ferreira IL, Pereira C, Oliveira CR, Rego AC. Amyloid-beta peptide 1-42 causes microtubule deregulation through N-methyl-D-aspartate receptors in mature hippocampal cultures. Curr Alzheimer Res. 2012;9(7):844-56.

40. Varela-Nallar L, Inestrosa NC. Wnt signaling in the regulation of adult hippocampal neurogenesis. Front Cell Neurosci. 2013;7:100.

41. Machon O, Backman M, Machonova O, Kozmik Z, Vacik T, Andersen L. A dynamic gradient of Wnt signaling controls initiation of neurogenesis in the mammalian cortex and cellular specification in the hippocampus. Dev Biol. 2007;311(1):223-37.

42. Faigle R, Song Hongjun. Signaling mechanism regulating adult stem cells and neurogenesis. Biochim Biophys Acta. 2013;1830(2):2435-2448.

43. Maschio DA, Oliveira RB, Santos MR, Carvalho CPF, Barbosa-Sampaio HCL, Collares-Buzato CB. Activation of the Wnt/β-catenin pathway in pancretic beta cells during the compensatory islet hyperplasia in prediabetic mice. Biochem Biphys Res Commun. 2016; 478(4):1534-40.

44. Chacón MA, Varella-Nallar L, Inestrosa NC. Frizzled-1 is involved in the neuroprotective effect of Wnt3a against Abeta oligomers. J Cell Physiol. 2008;217(1):215-27.

45. De Ferrari GV, Chacón MA, Barría MI, Garrido JL, Godoy JA, Reyes AE, et al. Activation of Wnt signaling rescues neurodegeneration and behavioral impairments inducd by beta-amyloid fibrils. Mol Psychiatry. 2003;8(2):195-208.

46. Chen Y, Bodles AM. Amyloid precursor protein modulates β-catenin degradation. J Neuroinflammation. 2007.10;4:29.

47. DaRocha-Souto B, Coma M, Pérez-Nievas BG, Scotton TC, Siao M, Sánchez-Ferrer P, et al. Activation of glycogen synthase kinase-3 beta mediates β-amyloid induced neuroritic damage in Alzheimer's disease. Neurobiol Dis. 2012;45(1):425-37.

48. Tseng BP, Green KN, Chan JL, Blurton-Jones M, LaFerla FM. Aβ inhibits the proteasome and enhances amyloid and tau accumulation. Neurobiol Aging. 2008;29(11):1607-1618.

49. Velazquez R, Shaw DM, Caccamo A, Oddo S. Pim1 inhibition as novel therapeutic strategy for Alzheimer's disease. Mol Neurodegener. 2016;11(1):52.